Influence of the equation of state for moderate to high pressure gaseous systems

M. Brateau, Steven Kerampran, A. Bouchama, A. Clough, M. Arrigoni

Influence of the equation of state for moderate to high pressure gaseous systems

M. BRATEAU,[1,2,a)] S. KERAMPRAN,[2] A. BOUCHAMA,[3] A. CLOUGH,[1] and M. ARRIGONI[2]
[1)] *CTA International, 7 route de Guerry, 18000 Bourges, FRANCE*
[2)] *ENSTA Bretagne, IRDL UMR-CNRS 6027, 2 rue F. VERNY, 29200 Brest, FRANCE*
[3)] *DGA Land Systems, Echangeur de Guerry, 18000 Bourges, FRANCE*

(Dated: 29 September 2024)

For transportation and defense systems, equations of state describe the thermodynamical behavior of gases, as a function of pressure, density and temperature and are often used to close systems of equation (such as Navier Stokes for fluid mechanics). For low pressure system (under a few dozen MPa), the ideal gas equation can be used, whereas for high pressure system (above 1,000 MPa), dedicated equations of state are used (Jones-Wilkins-Lee: JWL or Becker-Kistiakowsky-Wilson: BKW). For intermediate pressure systems, such as interior ballistics or pyromechanisms, where the pressure is around a few hundreds MPa and many phenomena interact closely and simultaneously (multiphysics system: combustion, fluid dynamics, thermics, fluid-structure interaction, thermodynamics...), the ideal gas equation is not valid anymore and nor are the JWL or BKW equations. A dedicated equation of state is then necessary for intermediate level of pressures, and its choice is not obvious. This paper presents a comparison of equations of state for this range of pressure (Noble-Abel, Van der Waals, virial), details the calculations of the involved coefficients and their effects on uncertainties and study the influence of the equation of state on the predictions of pressure, density, pressure coefficient and heat transfer, with both analytical and numerical approach. The results highlight the importance of the choice of the equation of state, especially for a multiphysics system, as the equation of state influences not only thermodynamical properties (pressure, density, temperature) but also thermical properties of a system, such as heat transfer.

Keywords: Interior ballistics, Equations of state, Gas dynamics, CFD

I. INTRODUCTION

In the transportation and defense industries, where systems combine thermodynamics and mechanics (thermic automotive motors, aeronautic and aerospace reactors, defense systems, pyromechanisms...) it is crucial to describe the evolution of thermodynamic values. For such systems, the prediction of these values (pressure, temperature and density) is given by an equation of state, abbreviated EOS in this paper, (1), which describes the behavior of three thermodynamical properties relatively to one another[1]. Such a relationship is most often required to close a system of conservation laws, such as the Navier Stokes equations for fluid mechanics. As it gives a macroscopic view of phenomena occurring at microscopic scales, an equation of state usually relies on physical assumptions which limit its range of validity in terms of thermodynamical properties. Furthermore, it implies the knowledge of a number of coefficients obtained either from experiments or from analytical calculations. Determining these coefficients can be arduous. The choice of an equation of state is therefore governed by the expected range of variation of the thermodynamical properties in the considered system. The frame of this work is not to develop a new equation of state for interior ballistics application, but to propose an existing one, that remain straightforward and can easily be used by engineers.

$$f(P, \rho, T) = 0 \tag{1}$$

At atmospheric conditions and in most industrial setups, the pressure is low (under a few MPa), allowing the use of the well-known ideal gas law. This equation has strong assumptions: point-like molecules and no interactions between them. These assumptions, which hold for low to moderate pressures, provide a straightforward equation which stands as a good reference for all other EOS[1]. When high pressures are encountered, dedicated EOS have to be used. A good example is given by the detonation of an explosive charge. In this instance, very high presures are observed (over 1,000 MPa). This has been the topic of extensive work since the late 40s, leading to the establishment of the JWL[2] (Jones-Wilkins-Lee) or BKW[3] (Becker-Kistiakowsky-Wilson) equations of state. Both these equations are semi-empirical and need several parameters (mostly empirical), which are tabulated[4]. The JWL EOS is adapted to high pressure regimes, whereas BKW is better for intermediate and high pressure[5]. For intermediate levels of pressure (of the order of a few hundreds of MPa), the choice of an equation of state is not obvious. Indeed, this is the range of pressure where the ideal gas equation is inaccurate and where the EOS for detonics (high pressure) are needlessly convoluted and not especially adapted. Such

[a)] Electronic mail: marion.brateau@ensta-bretagne.org

conditions can for instance be encountered in interior ballistics. Essentially, interior ballistics is the study of the phenomena happening in a gun when it is firing. It can also be extended to some pyromechanisms (ie. mechanisms operating thanks to a propellant charge, such as some release systems in aerospace or airbags in vehicles). The functioning of a weapon is relatively straightforward: an energetic material (propellant) is ignited in a closed vessel, producing a large volume of gas in a short time, which drives a projectile outside a barrel[6–8]. This system is highly multiphysics as several phenomena interact simultaneously (combustion, heat transfer, chemistry, dynamic behavior of materials and structures and fluid-structure interaction are involved) for a short duration (a few milliseconds). The ranges of pressure, density and temperature are also unusual (respectively several hundreds of MPa, several hundreds of $kg \cdot m^{-3}$, several thousands of Kelvins).

This choice of the equation of state is crucial though, as it directly influences the prediction of the thermodynamic values in the system, and therefore the performance previsions of a weapon. As the system involves many coupled phenomena, the influence of the equations of state extends beyond the mere prediction of its thermodynamic behavior. Quantifying the consequences of the choice of an equation of state on all physical values (both thermodynamic and non-thermodynamic) is therefore a point of interest. The ideal gas equation is not valid for an interior ballistics application, and the well-known equations of state for detonics (JWL, BKW...)[2,3] are too convoluted, besides the parameters are semi-empirical so they would not be adapted for the interior ballistics conditions. Indeed, the assumptions of the ideal gas are not respected (point like molecules and no interactions), and there is no detonation in interior ballistics (chemical reactions are not driven by a shock wave). In many interior ballistics model, the reference equation of state is the Noble-Abel equation[9]. This equation has been used for decades[3,7,8] and is implemented in many interior ballistics codes (both commercial and academic). However, the development of modern weapon systems has set a trend leading to the increase of functioning pressures. The Noble-Abel equation of state may be outdated for such systems. Some authors therefore recommend the use of other equations of state (Van der Waals, virial) for the range of pressure of interior ballistics[10–12]. However, to the authors knowledge, no open literature offers a proper discussion about the uncertainties induced by the choice of such EOS.

The aim of this paper is to study the predictions of the physical values of an intermediate pressure system (with an application to interior ballistics) depending on the equation of state chosen to describe the behavior of the gas. Firstly, the prediction of the pressure is studied through an analytical approach, comparing four equations of state: ideal gas, Noble-Abel, Van der Waals and the virial equation. Uncertainties induced by the EOS choice are interpreted through the mathematical formalism of interval analysis. Secondly, a numerical approach based on CFD (Computational Fluid Dynamics) has been used to study the multiphysics part of the problem. The commercial software used is STAR-CCM+©(version 16). This study focuses on the influence of the equation of state on thermal and aerodynamical properties of a fluid flowing around a thick airfoil.

The gaseous mixture considered in the study (except for the last section on combustion products) is air (molar fraction : $21\%O_2$ and $79\%N_2$). This gas has been chosen for its simplicity (only two components) and has been extensively studied in the open literature. The work can easily be extended to a mixture representative of combustion products, as done in the last section.

II. INFLUENCE OF THE EQUATION OF STATE ON THE PREDICTION OF THERMODYNAMIC VALUES

The equation of state allows the prediction of a thermodynamical value knowing two others. In this study, the pressure is predicted depending on the equation of state, as a function of the density and the temperature is arbitrary fixed at a value representative of a flame temperature (around 2500K). The determination of the coefficient for each equation of state is also described (for a single component gas and for gaseous mixtures).

1. Considered equations of state (EOS)

The first equation of state studied is the ideal gas equation (2). This equation of state is the simplest one as only a single parameter of the gas is needed: the molecular weight, needed for the determination of r, which is the ideal gas constant ($R = 8.314\ J \cdot mol^{-1} \cdot K^{-1}$) divided by the molecular weight. This parameter is easily accessible and well-known. For a gaseous mixture, a simple mean molecular weight is used, weighted by the mass fraction of each component. The assumptions of this equation are highly restrictive: the volume of the molecules composing the gas and the interactions between the molecules are neglected. This is valid when the pressure and density of the gas are relatively low[1,3] (under a few MPa). This EOS is too restrictive for high pressure applications, but its simple expression constitutes a basis for establishing many other EOS (including Noble Abel and Van der Waals EOS) and is therefore included in this study as a reference.

$$P = \rho \cdot r \cdot T \tag{2}$$

The Noble-Abel equation is widely used in interior ballistics[6–8] and is recommended by a NATO reference document: STANAG 4367[9]. This equation (3) is an improvement of the ideal gas equation, introducing the volume occupied by the molecules with the parameter η, the covolume (4). However, the interactions between

the molecules are not represented. Two parameters are needed for this equation: the molecular weight and the covolume. The determination of the latter can be achieved with a thermochemical software or closed vessel tests (Amagat's method[13]). This experimental device is mostly used for the determination of the covolume of gases produced by the combustion of propellant. Analytical determination is also possible (4), as the covolume is a function[14] of the critical pressure (P_c) and critical temperature (T_c). For a gaseous mixture, a mean covolume weighted by mass fraction of the components is used. The uncertainties on the covolume depend on the method used to evaluate it but are usually restricted to a few percent (accounting for the experimental accuracy or the precision on the values of P_c and T_c).

$$P = \frac{\rho \cdot r \cdot T}{1 - \rho \cdot \eta} \tag{3}$$

$$\eta = \frac{r \cdot T_c}{8 \cdot P_c} \tag{4}$$

The Van der Waals equation of state (5) is a correction of the Noble-Abel equation in order to consider the interactions between molecules composing the gas at short range (repulsion) and long range (attraction). The interactions between the molecules are considered with the parameter a (consequence of the Van der Waals bond). Three parameters are needed for this equation: the molecular weight, the covolume and the interaction term a (6). Like the covolume, a is a function of the critical pressure and temperature[14]. MA et al[11] recommend this equation for an interior ballistics application, as the interaction term should add a better description of the behavior of the gas. However, adding a parameter also adds uncertainties. A mixing law must be used to evaluate this coefficient for a gaseous mixture (quadratic mean as proposed in[14]).

$$P + \frac{a}{\rho^2} = \frac{\rho \cdot r \cdot T}{1 - \rho \cdot \eta} \tag{5}$$

$$a = \frac{27 \cdot r^2 \cdot T_c}{64 \cdot P_c} \tag{6}$$

The virial equation is a limited expansion (7), at the second order in this paper (the coefficients for the higher orders are especially difficult to calculate[1]). NERON and SAUREL[10] use the virial at the first order. The authors of[1,3,12] advocate for this equation when the pressure and temperature are in the interior ballistics range (respectively above 300 MPa and 2000 K). As for the Van der Waals equation, three parameters are needed: the molecular weight, B and C. These two parameters represent the interactions respectively between two molecules (B) and three molecules (C). The main difference between the virial coefficients and the coefficients of the other considered equations is the temperature dependence. Indeed, the virial coefficients are temperature dependent, and their method of calculation is described in the next paragraph. The mixture law needed for a gaseous mixture is also described in the next paragraph. The uncertainties linked to these coefficients are above 10%, which is higher than for the other equations of state[1,15].

$$P \approx \rho \cdot r \cdot T(1 + B\rho + C\rho^2 + \dots) \tag{7}$$

The method of calculation of the virial coefficients, B and C is described in[1]. The coefficients are integral functions of the intermolecular potential and the temperature. The expression of the coefficient B is given (8) (N the Avogadro number, k the Boltzmann constant, T the temperature, s the position of the molecule, φ the intermolecular potential):

$$B(T) = 2\ \pi\ N \int_0^\infty (1 - e^{(-\varphi(s)/kT)\ })\ s^2\ ds \tag{8}$$

The expression of the third coefficient C is of the same nature as for B. It is not reproduced in this paper, as the formula is convoluted and gives no supplementary information, but its expression is given in[1]. The determination of the virial coefficients therefore implies the choice of an intermolecular potential φ for every component of the gas. For non-polar molecules, the Lennard-Jones "6,12" potential has been used as recommended in[1], as expressed in (9). This model relies on the hard sphere model, which is not strictly accurate but considerably simplifies the calculations. The Lennard-Jones potential (9) is only a function of the position of the molecules (radius r) and two constants are needed (the size of particle σ and the dispersion energy ε), which are available in the literature for many gases[1]. The constant σ represents the distance at which the value of the potential is zero and ε is the depth of the potential well (homogenous to an energy). Uncertainties are introduced with the values of these constants, approximately 10%[1].

$$\varphi(r) = 4\ \varepsilon\ [\frac{\sigma^{12}}{r^{12}}\ - \frac{\sigma^6}{r^6}] \tag{9}$$

In this study, the components of the gas are only non-polar molecules (N_2 and O_2), so the Lennard-Jones potential is applicable. However, for non-polar molecules, such as gaseous water (usually one of the main components of combustion products), another potential should be substituted. The Stockmayer potential is often used[1,15] and allows the consideration of the polarity of the molecules. More details are available in[16] and are not reproduced in this paper as this potential has not been used for air. Besides uncertainties of the constants of the potential, mathematical simplifications are proposed in[1] leading to the series expansion of B and C.

Coefficients b_j and c_j are tabulated in[1]. Computed in the 1960s with the numerical tools of the time, there are most likely uncertainties on these coefficients, although a numerical verification of the b_j coefficients performed in the frame of this work with actual method has led to the same results as[1].

$$B(T) = \ b_0 \cdot \sum_j b_j (\frac{kT}{\varepsilon})^{-(2j+1)/4} \tag{10}$$

$$b_0 = \frac{2}{3}\pi N \sigma^3 \tag{11}$$

$$C(T) = b_0^2 \cdot \sum_j c_j (\frac{kT}{\varepsilon})^{-(j+1)/2} \tag{12}$$

These expressions allow the calculations of the coefficients for a single constituent and can be used to determine the corresponding parameters for a gaseous mixture. Two mixing laws are proposed in the STANAG 4400[15]. The first is an intuitive one, based on the ponderation of the coefficients of the single components by mass fractions (wi). This law has been introduced by Corner[7] and eases the calculations, as it neglects the interactions between molecules.

$$B(T) = \sum_j w_j \cdot B_j \tag{13}$$

$$C(T) = \sum_j w_j \cdot C_j \tag{14}$$

The second law is considerably more complex, since it considers interactions between all the molecules composing the mixture. This mixing law only applies to the calculation of second virial coefficient B as the STANAG 4400[15] states that the complex mixing law for C is too complicated and the simple law gives sufficiently accurate results for this parameter. The expression of the contributions of the interaction for B is equation 15

$$B(T) = \frac{\sum w_a \cdot w_b \cdot B_{ab}}{\sum w_i^2.} \tag{15}$$

The interaction coefficient B_{ab} is calculated with averaged Lennard-Jones potential coefficients (eq 16 arithmetic mean for σ and quadratic mean for ε). The calculation for B_{ab} uses equation 10, but with σ_{ab} as σ and ε_{ab} as ε.

$$\sigma_{ab} = \frac{\sigma_a + \sigma_b}{2}; \varepsilon_{ab} = \sqrt{\varepsilon_a \cdot \varepsilon_b} \tag{16}$$

2. Equations of state's comparisons with coefficients from the literature

As previously detailed, the determination of the parameters of the equations of state can be challenging, especially for a mixture. A first comparison between the four equations of state (ideal gas, Noble-Abel, Van der Waals and virial) has been done with parameters provided by the literature[17] (given in table I). Experimental values from the SESAME database for air (table 5030) have been used as validation[18]. The virial coefficients in[17] given at a temperature of 2500K (close to most propellants flame temperature), whereas the SESAME database's temperature is 2611.13K. It should be noted that the range of temperature covered by the SESAME database is wide for air: the temperature gap between two entries in the table for the range of interest is over 1000K. It therefore made little sense to perform an interpolation between two values to obtain a validation point at 2500K, as it would have implied too large uncertainties. Another limitation of the SESAME database is the low number of points in the range of interest (classical range of pressure of interior ballistics: 300 MPa – 700 MPa). Despite these limitations, the SESAME database still gives a good reference for the comparisons of the different equations of state.

TABLE I. Values of the equations of state coefficient for air from the literature[17,19]. The virial coefficients are taken at 2500K.

Coefficients	Values	Units
Covolume η	$1.3 \cdot 10^{-3}$	$m^3 \cdot kg^{-1}$
Interaction term a	173.2	$Pa \cdot m^6 \cdot kg^{-2}$
B (2500K)	$1.0 \cdot 10^{-3}$	$m^3 \cdot kg^{-1}$
C (2500K)	$0.9 \cdot 10^{-6}$	$m^6 \cdot kg^{-2}$

Figure 1 shows the pressure plotted as a function of the density for the considered equations of state. The black crosses represent the SESAME database (5030 for air), and the grey part of the graph is the interior ballistics range of pressure.

For moderate densities, all the equations of state predict approximately the same pressure (less than 10% of difference under 100 $kg \cdot m^{-3}$, the difference reducing when the density decreases). This behavior is explained by the fact that the assumptions of the equations of state become equivalent at low density (the deviations from an ideal gas behavior appears at a higher density, essentially the average distance between molecules becomes too small for the ideal gas equation to be valid). The results obtained with the Noble-Abel and Van der Waals equations are close to each other, with relative deviations lower than 5%. It appears that the corrections of the interaction term (a parameter) in the Van der Waals equation has a relatively weak influence for air as a gaseous mixture of O_2 and N_2. For the rest of this study, the Van

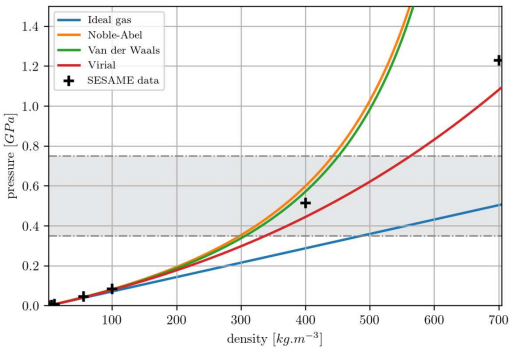

FIG. 1. Pressure as a function of density for air at 2500K predicted by different equations of state. Coefficients for the EOS are given in table I. The grey area highlights the pressure range commonly considered in interior ballistics applications. Crosses are experimental validation data extracted from the SESAME database (5030)[18].

der Waals equation has been excluded as it gives similar results as the Noble-Abel equation. Another singularity is the vertical asymptote of both these equations when density increases (above 500 $kg \cdot m^{-3}$). This nonphysical behavior is an issue, as it does not predict accurately the evolution of the pressure at high density, especially when the pressure is close to the upper boundary of the interior ballistics range. This divergence is caused by the mathematical formalism of the Noble-Abel and Van der Waals EoS (division by zero when the specific volume is close to the covolume). With the permanent demand of weapons with better performances, the maximal chamber pressure tends to increase, leading to higher mispredictions when using the Noble-Abel equation. This divergence is so pronounced that, above 600 $kg \cdot m^{-3}$, the ideal gas equation of state becomes a better option than the Noble-Abel or Van der Waals equations. However, the ideal gas equation is not adapted to high pressure and density gases for physical reasons (its assumptions are not valid anymore). If considering only the predictions of pressure as a function of density at a given temperature, the ideal gas equation of state can reasonably be used up to 100 $kg \cdot m^{-3}$.

From this study, the virial equation of state with coefficients from the literature stands out with its stability and proximity to the SESAME database (5030). However, uncertainties on these coefficients have not been found explicitly in the literature. Subsections II 3, II 4 and II 5 focus on the calculations of the EOS coefficients and introduces a method to estimate the uncertainties of the coefficients. This gives also a global uncertainty on the pressure predictions given by the EOS.

3. Covolume calculations

This section presents the calculation of the covolume of air from the critical pressure and critical temperature (4). As for the virial coefficient, the covolume of each component is calculated, then a resulting covolume is obtained using a mixing law (mean-weighted by molar fractions). For air, the calculations are straightforward, as there are only two components to consider. The values of the critical pressure and critical temperature are given by[20,21] along with their uncertainties, estimated by[22]. Table II presents the covolume for air, N_2 and O_2.

TABLE II. Values of the critical pressure and temperature of N_2[20] and O_2[21] for the calculation of the covolume for air using (4)

Components	P_c (kPa)	T_c (K)	Covolume $\eta(kg \cdot m^3)$
N_2	33.98 ± 0.007	126.19 ± 0.100	$1.38 \cdot 10^{-3}$
O_2	50.43 ± 0.005	154.88 ± 0.001	$0.99 \cdot 10^{-3}$
Air	-	-	$\mathbf{1.29 \cdot 10^{-3}}$

The covolume calculated is close to the one found in the literature (difference less than 1%, as the covolume of the literature is $1.30 \cdot 10^{-3} m3 \cdot kg^{-1}$). The uncertainties linked to the parameters needed for the calculations are extremely low (less than 0.1% at most), giving a low uncertainty of the final coefficient. A comparison between the uncertainties of the coefficients for the Noble-Abel and the virial equations has been done and is presented section II 5.

4. Virial coefficients calculations

This section presents the virial coefficient calculations for air as a binary mixture of oxygen and nitrogen (respectively 21% and 79%). Both these molecules are nonpolar molecules, so the Lennard-Jones intermolecular potential has been used. The potential coefficients for each component are given in table III. σ represents the value where the potential is null, ε is the depth of the potential well, k is the Boltzmann constant (ε/k is easily found in the literature). However, air being a mixture, a mixing law is necessary to obtain the relevant coefficients. The two mixing laws presented above have been compared in this study. To be consistent with the SESAME database and allow a more accurate comparison, the calculations have been done at 2611.13 K (the database temperature).

The uncertainties of the Lennard-Jones coefficients are estimated at 10 %[1,15], which is higher than the uncertainties on the covolume. These uncertainties impact the final value of the virial coefficients, for both the components and the mixture. A study on the uncertainties is available section II 5. The coefficients for each component and the interaction coefficient (complex mixing law for the second coefficient B) are given in table IV.

TABLE III. Values of intermolecular potential (Lennard-Jones) for N_2 and O_2[1]. These values are needed to calculate the virial coefficient of both these molecules and air.

Components	σ (nm)	$\frac{\varepsilon}{k}$(K)
N_2	0.358	118
O_2	0.370	95

This interaction coefficient, representing the interactions between N_2 and O_2 has the same magnitude as the coefficient for the single components. This accounts for the notable difference (20%) between the mixing laws used for the virial coefficient B (table IV), as the interaction term is not neglectable.

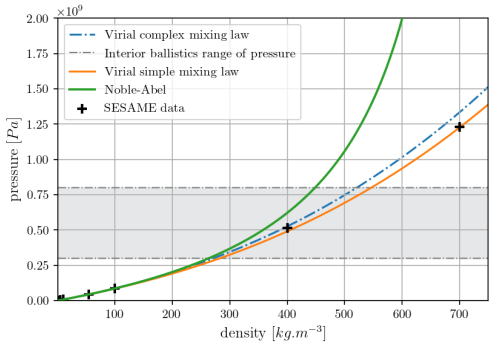

FIG. 2. Pressure as a function of density for air at 2611.13K predicted by Noble-Abel and the virial, for two mixing laws for virial (simple and complex). Coefficients for the EOS are given in table II for Noble-Abel and table IV for virial. The grey area highlights the pressure range commonly considered in interior ballistics applications. Crosses are experimental validation data extracted from the SESAME database (5030).

The results obtained with the virial equation of state using both sets of coefficients (obtained respectively with the simple and complex mixing laws) are plotted figure 2, along with those derived from the Noble Abel equation. The SESAME database (5030) is still used as a reference (black crosses). The mixing laws are relatively close at moderate density (under 200 $kg \cdot m^{-3}$). The difference increases but remains under 10% at 700 $kg \cdot m^{-3}$. It should also be noted that at the highest density for the SESAME point, the simple mixing law is more accurate with respect to the reference data than the complex one. It is highly probable that the SESAME database, which is both an empirical and analytical database, uses a simple mixture law for the results at high densities. For a simple gaseous mixture such as air, the calculations for the complex law are quite straightforward. However, for a multi-component mixture (such as combustion products), the calculations become laborious as it multiplies the interactions terms. This study highlights that the use of the simple mixture law for the virial coefficients seems to be suitable.

5. Uncertainties

One of the difficulties when using an equation of state is to determine the coefficients of the equation, as seen previously. The determination can be made either from experiments or analytical calculations and induces uncertainties on the equations of state, which are not often quantified. For the covolume (parameter of the Noble-Abel equation of state) the main uncertainties are on the values of the critical pressure and critical temperature (under 0.1% in the worst case, estimated by the Thermodynamics Research Center[22] in table II or on the pressure gauges sensitivity when the covolume is determined experimentally (for combustion products, for example). In this section, the covolume is calculated using the critical pressure and temperature. For the virial equation, the intermolecular potential parameters ($\sigma, \varepsilon \ldots$) are the main sources for uncertainties. These are estimated at 10% for each parameter[1,15]. Interval analysis[23,24] has been used to compute the uncertainties on the coefficients of equations of state. This mathematical formalism relies on the set theory to describe interval of uncertainties around the exact value. Indeed, most of the values used in physics are not precisely known (irrational number like π, measured quantities, numerically calculated values...). They are given with uncertainties, which can be expressed with intervals. Let's consider a physical quantity m, which has uncertainties. It is then possible to write:

$$m_1 \leq m \leq m_2 \tag{17}$$

Another way of writing the relation (17) is to write it with an interval form (18):

$$m \in [m_1; m_2] \tag{18}$$

The quantity m belongs to the interval given in eq 18, which has a lower bound (m_1) and an upper bound (m_2). Considering now that m is linked to a relation (for example, the density formula, $\rho = m/V$), the uncertainties on m will be transmitted to the final result through this relation (the density in our example). Most of the physical relations are described with more than one coefficient with uncertainties. When several coefficients are linked by a relation, there are several intervals interacting mathematically with arithmetic operations (addition, multiplication...). The arithmetic of interval is described in many references[23,24] and set the rules of mathematical manipulations of intervals.

As an example, let's consider the density (19) as a quotient of the mass (18) and the volume (20):

TABLE IV. Values of the virial coefficients (B and C) for N_2, O_2 and air, depending on the mixing law (simple and complex). The simple law is a mass fraction weighted average of the coefficient whereas the complex law accounts for the interactions between the components of the mixture.

Components	$B_{simple}(m^3 \cdot kg^{-1})$	$B_{complex}(m^3 \cdot kg^{-1})$	$C\ (m^6 \cdot kg^{-2})$
N_2	$1.17 \cdot 10^{-3}$	$1.17 \cdot 10^{-3}$	$1.10 \cdot 10^{-6}$
O_2	$1.06 \cdot 10^{-3}$	$1.06 \cdot 10^{-3}$	$0.96 \cdot 10^{-6}$
N_2-O_2 interactions	-	$1.11 \cdot 10^{-3}$	-
Air	$\mathbf{1.15 \cdot 10^{-3}}$	$\mathbf{1.44 \cdot 10^{-3}}$	$\mathbf{1.07 \cdot 10^{-6}}$

$$\rho = \frac{m}{V} \tag{19}$$

$$V \in [V_1; V_2] \tag{20}$$

Then, it is possible to determine the uncertainties on the density (21).

$$\rho \in [\frac{m_1}{V_2}; \frac{m_2}{V_1}] \tag{21}$$

In this paper, interval analysis has been used to compare the uncertainties linked to the calculation of the coefficients for the equation of state. For the Noble-Abel equation, the uncertainties are extremely low (maximum 0.1%), allowing a narrow interval for the covolume of each component of the mixture (N_2 and O_2 in that case), therefore a narrow interval for the covolume of air. The expressions of the maximal and minimal covolume are given in (22) and (23). The numerical values resulting from the calculations are available in (24). These values have been used to calculate the pressure predicted by Noble-Abel with the minimal and maximal covolume. This gives an interval where the pressure is with certainty.

$$\eta_{min} = \frac{Pc_{min}}{8 \cdot r \cdot Tc_{max}} \tag{22}$$

$$\eta_{max} = \frac{Pc_{max}}{8 \cdot r \cdot Tc_{min}} \tag{23}$$

$$\eta \in [1.29 \cdot 10^{-3}; 1.298 \cdot 10^{-3}] m^3 \cdot kg^{-1} \tag{24}$$

The interval for the covolume allows to plot the Noble-Abel equation with its range of uncertainties (figure 3). The interval gives the maximal and minimal values of the covolume, which are used to plot the evolution of the pressure as a function of the density (fixed temperature) for the Noble-Abel equation. It gives a range, where the accurate predicted pressure is with certainty (colored part of the graph figure 3).

For the virial coefficients, the uncertainties mainly stem from the uncertainties on the intermolecular potential, which can be expressed with intervals (as for the covolume, $\sigma \in [\sigma_{min}; \sigma_{max}]$ and $\varepsilon \in [\varepsilon_{min}; \varepsilon_{max}]$). These intervals are then used to calculate the maximal and minimal values of B (25 and 26) and C (27 and 28) for each component of the mixture. The mixture law is then applied to find the resulting maximal and minimal coefficients (29 and 30 for the numerical values). Because of the wider range of uncertainties, especially on the intermolecular potential parameters, the virial coefficients eventually exhibit large uncertainties. This in turn confers a quite wide global uncertainty on the results obtained with the virial equation, meaning that the prediction of the pressure from the virial equation of state is not as accurate as the prediction with the Noble-Abel equation.

$$B_{max}(T) = \frac{2}{3}\pi N \sigma_{max}^3 \cdot \sum_j b_j (\frac{kT}{\varepsilon_{min}})^{-(2j+1)/4} \tag{25}$$

$$B_{min}(T) = \frac{2}{3}\pi N \sigma_{min}^3 \cdot \sum_j b_j (\frac{kT}{\varepsilon_{max}})^{-(2j+1)/4} \tag{26}$$

$$C_{max}(T) = (\frac{2}{3}\pi N \sigma_{max}^3)^2 \cdot \sum_j c_j (\frac{kT}{\varepsilon_{min}})^{-(j+1)/2} \tag{27}$$

$$C_{min}(T) = (\frac{2}{3}\pi N \sigma_{min}^3)^2 \cdot \sum_j c_j (\frac{kT}{\varepsilon_{max}})^{-(j+1)/2} \tag{28}$$

$$B \in [0.77 \cdot 10^{-3}; 1.64 \cdot 10^{-3}] m^3 \cdot kg^{-1} \tag{29}$$

$$C \in [0.49 \cdot 10^{-6}; 2.16 \cdot 10^{-6}] m^6 \cdot kg^{-2} \tag{30}$$

The results obtained with the virial equation are treated in a similar way as the ones derived with the Noble Abel equation. The interval gives the maximal and minimal values of the virial coefficients, which are used to plot the evolution of the pressure as a function of

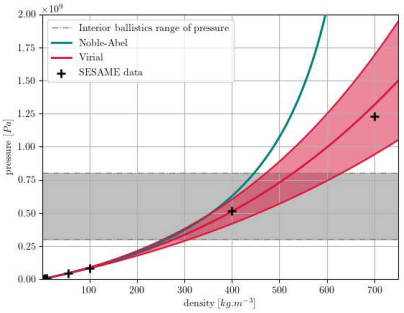

FIG. 3. Pressure as a function of density for air at 2611.13 predicted by different equations of state, along with their respective intervals of uncertainties (Noble-Abel uncertainties are too thin to be seen on the figure). The grey area highlights the pressure range commonly considered in interior ballistics applications. Crosses are experimental validation data extracted from the SESAME database (5030).

the density (fixed temperature) for the virial equation. The resulting range (colored part of the figure 3) is a prediction of the pressure.

Figure 3 is a plot of the pressures calculated with both equations of state, with their respective intervals of uncertainty (the representation is a tube around the curve). The reference SESAME data are also plotted. It should be noted that these points have low uncertainties (less than 1%[25]), which are not represented here. As highlighted previously, the virial equation has a large range of uncertainty, whereas the Noble-Abel range is extremely narrow (to the point where it is actually not visible on figure 3 with respect to the virial equation range of uncertainty). For the lower interval of pressure encountered in interior ballistics (between 300 MPa and 500 MPa) the pressure obtained with the Noble-Abel equation is included within the range of uncertainties of the pressure calculated with the virial equation. Above a density of 400 $kg \cdot m^{-3}$, the difference between the pressures derived from both equations is noticeable, as the vertical asymptote of the Noble-Abel equation progressively deteriorates the results and leads to increasing deviations from the reference points (SESAME data). Nonetheless, there is only one reference point in the range of pressure of interest for interior ballistics. It is then difficult to conclude with certainty, as more reference points would have been required. The choice of the equation of state for intermediate level of pressure is therefore not obvious and the uncertainties of the EOS coefficients play an important part in the choice. This part has been focused on the thermodynamical predictions of an intermediate level pressure system. However, the impact of the choice of the EOS on other physical quantities is not well-known and has been investigated. The results of this study is presented section III.

III. INFLUENCE OF THE EOS ON NON-THERMODYNAMICAL PROPERTIES (AERODYNAMICS AND THERMICS): NUMERICAL APPROACH

The EOS plays an obvious part in thermodynamical and thermochemical phenomena, but its influence on other physical mechanisms (in which thermodynamics apparently play a lesser part, such as aerodynamics or thermics) can be more difficult to ascertain. Furthermore, interior ballistics phenomena are highly interdependent and involve many physical domains. The choice of the EOS can therefore influences more widely the physical quantities of a system, especially when the system is highly multiphysics (interior ballistics for instance). To evaluate this influence, an academical case is numerically studied in this part with a CFD approach. The numerical work aims to study the influence of the EOS on the prediction of other physical phenomena.

The simulations should remain straightforward to analyze, which excludes reactive systems and combustion models. However, as the study considers the multiphysical coupling in interior ballistics, the monitored phenomena must be chosen adequately. In this study, the thermic and aerodynamic properties of a fluid flowing around an object are studied. The case of study should also exhibits pressure gradients in the flow, in order to analyse the possible influence of the EoS on these gradients. This pointed towards the flow around an immerged body. Three equations of state have been compared in this study: ideal gas, Noble-Abel and the virial. For the purpose of the study, the chosen case should enable to highlight the differences between the considered EOS. Since they yield similar results for low to moderate pressures, a relatively high pressure (300 MPa) and high temperature (2000 K, which is at the lower bound of the interior ballistics range of temperature) flow is considered, close to the interior ballistics conditions. Ideally, the test configuration should also be sufficiently common to be documented in the literature to allow comparisons, and free from any confidentiality issues.

The choice has been made to study the flow around a thick airfoil (NACA 0020). This body has been chosen for its property of symmetry, its ability to produce a steady flow (for an adequate Reynolds number , estimated between $1 \cdot 10^6$ and $2 \cdot 10^6$ for NACA 0012[26]. In this case $Re = 6 \cdot 10^6$ and the profile is a NACA 0020), and the quite extensive literature available for this airfoil[27–29]. The gas studied is air, chosen for its simplicity (only two components) and its well-known behavior. To prevent shock waves, which would have interfered with the flow (discontinuity of pressure, density...), the flow velocity has been chosen to maintain a subsonic flow (Mach number arbitrarily set around 0.3 in the study). The flow is steady and laminar, as introducing a tur-

bulence model would have vainly complicated the simulations. The chosen configuration does not represent conditions likely to be encountered in any actual setup, and is strictly academical as stated previously. Its sole purpose is to evidence the differences on the prediction of physical quantities depending on the equation of state. Quantitative values derived from the simulations should be considered with care, since they would require validation (which would be hard to obtain, given the peculiarity of the considered flow).

The CFD software STARCCM+©, based on finite volume method, (version 16) was used for the study. The chord's length of the airfoil is arbitrary 1m long. The airfoil has a wall boundary condition, assigned with a constant temperature (300 K, 1000 K or 1500 K depending on the configuration). The computational domain has been designed to be larger than the airfoil to avoid side effects (rectangle, 20m*40m). All the presented simulations are two-dimensions steady-state simulations. A symmetry condition has been used on the bottom half of the airfoil and the domain, allowing a reduction of the mesh domain. The flow enters on the left side of the domain, exits on the right side and the upper part of the domain. Figure 4 summarizes the configuration studied.

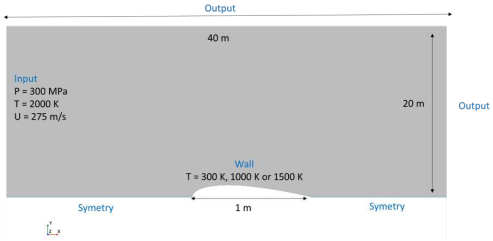

FIG. 4. Numerical configuration studied, with boundary and initial conditions, geometry of the domain and the airfoil.

The fluid considered is air (21% O_2 – 79%N_2) and enters the domain at 2000 K and 300 MPa (values sufficiently high to witness a difference between the equations of state and close to interior ballistics' conditions), its velocity is 275 $m \cdot s^{-1}$. The numerical integration model is a Riemann steady-state implicit with a Roe solver, with a second order space discretization. The ideal gas equation of state is natively implemented in STARCCM+©, but Noble-Abel and the virial are not. They have been implemented using field functions. The method is the same for all CFD software: users compute the expression of the density along with its derivative with respect to pressure and temperature. The expressions are detailed in the appendice.

Regarding the far field values (far from the airfoil) slight variations have been witnessed on the values of density, velocity and temperature of the domain (far from the foil), due to the chosen EOS. The far field values of temperature, pressure, density and velocity are given for each equation of state in table V. The far field values are the same for all configurations (temperature of the foil: 300K, 1000K or 1500K). The explanation is that the boundary conditions in STARCCM+©use ideal gas instead of the implemented equation of state, which induces difference when the EOS is not ideal gas.

TABLE V. Far field values (temperature, density and velocity) for each equation of state.

Far field values	Ideal Gas	Noble-Abel	Virial
Temperature (K)	2000	1975	1981
Density ($kg \cdot m^{-3}$)	523	313	344
Velocity ($m \cdot s^{-1}$)	269	349	333

It is then delicate to compare the results of the equations of state studied. The choice has then been made to work with dimensionless number, which allow a better comparison of the results.

The physical quantities monitored for the aerodynamic study are the pressure and the density around the airfoil, which allow to study the pressure coefficient (31), which is a dimensionless number. The "inf" indice indicates a far field value, P being the pressure ρ the density and V the velocity of the fluid. The effects of viscosity are also studied with the resulting force along the x-axis (total, contribution of pressure and contribution of shear).

$$C_p = \frac{P - P_{inf}}{0.5 \cdot \rho_{inf} \cdot V_{inf}^2} \tag{31}$$

To complete the study, the variation of a thermic property depending on the equation of state has been investigated. The chosen property is the heat flux, called q, which is the integral of the heat on the surface of the airfoil. C_{cal} is the calorific capacity, supposed constant in the paper, u_T is the transverse velocity, T is the temperature around the airfoil, T_{inf} is the far field temperature, T_+ is an dimensionless number, which expression is given in[30].

A normalization of the heat flux has also been performed (33), to allow a better comparison between the equations of state, called in this paper "heat transfer coefficient". The factor h, heat transfer coefficient for convection, is arbitrarily chosen at 10, as it is the magnitude for natural convection in air[31] and the intrinsic value of h is of no importance as long as the same value is used for all the configurations. The surface is 1 m^2. The prediction of the far field temperature depends on the equation of state (as stated in the beginning of the section), and the temperature of the surface of the airfoil depends on the configuration studied.

$$q = \frac{\rho \cdot C_{cal} \cdot u_T \cdot (T_{inf} - T)}{T_+} \tag{32}$$

$$C_{th} = \frac{q}{h \cdot S \cdot (T_{inf} - T)} \tag{33}$$

The final value of heat flux and forces along the x-axis fluctuate (purely numerical oscillations), so the values presented are the mean on the last 1000 iterations, along with the associated standard deviations (uncertainty of one sigma for the error bars).

The mesh has been refined to obtain an optimal configuration, both in term of calculation's duration and results' precision: the boundary layer has been meshed with 30 layers in its thickness ($\delta = 1.5 \cdot 10^{-5} m$) and the rest of the domain has been meshed with polygonal elements (size = 1 cm). Three configurations have been studied. The parameters of the study are the temperature of the airfoil: 300K (configuration 1), 1000K (configuration 2) and 1500K (configuration 3).

1. Verifications

Analytical verifications have been performed in the frame of this work, with the ideal gas equation as the relations are simple and well-known and for configuration 1. In particular, the pressure and temperature on the leading edge (P_0 and T_0) have been verified for an ideal fluid (inviscid, ideal gas), allowing the validation of both the pressure and the temperature (34 and 35). The Mach number is noted M, γ is the adiabatic coefficient (1.4 for a diatomic gas such as air).

$$\frac{P_0}{P} = (1 + \frac{\gamma - 1}{2} * M^2)^{\frac{\gamma}{\gamma - 1}} \tag{34}$$

$$\frac{T_0}{T} = (1 + \frac{\gamma - 1}{2} * M^2) \tag{35}$$

The results of the calculations are in good agreement with the simulations (less than 0.03% of difference). The pressure coefficient is a classical aerodynamical property (31). It is a normalization of the pressure along the airfoil. Two references have been exploited[27,28] to compare the pressure coefficient given in the literature and the pressure coefficient in the simulations.

As the chosen airfoil is well-known, the pressure coefficient in particular is studied in other papers for similar configurations[27,28] (NACA 0020 airfoil, Re = $2.7 \cdot 10^6$, for incompressible flow). The results[27,28] have been plotted in figure 5 and highlight the good agreement between the literature and our simulations. The differences observed between the simulations of this paper and the references are explained by the compressibility effects. Indeed, compressibility effects impacts the pressure coefficients[32]. The oscillations on the extrados are numerical.

Verifications of density on the first iterations of the users implemented EOS (Noble-Abel and virial) have been done. The density predicted by the calculations from the analytical expression of the EOS and the initial conditions is the same as the density predicted by the numerical simulation (identical values) on the first iterations. The manually implemented EOS seems to work correctly.

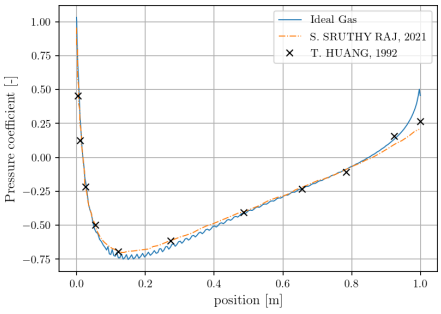

FIG. 5. Pressure coefficient as a function of position along the wing profile for the ideal gas equation, comparison with data from the literature[27,28] (similar magnitude of Reynolds number 10^6). Mach number: 0.3, temperature of the airfoil: 300K.

2. Aerodynamic properties

The pressure does not vary drastically around the foil (variations under 7%, figure 6). Furthermore, the pressure's predictions are also the same for each equation of state within a configuration, contrary to the density (figure 7), which depends on the equation of state (the variation are exclusively on the density, as the pressure is almost constant around the foil and the temperature is assigned to the foil). As a consequence, the predictions of pressure are independent of the configuration tested (temperature of the foil: 300K, 1000K and 1500K). The pressure is then not the good physical values to monitor the predictions of the equations of state. The pressure coefficient has been chosen instead.

The prediction of the pressure coefficient is then very similar for each equation of state (due to the normalization). The predictions are also in good agreement with the results from the literature[27,28].

In definitive; as highlighted by figure 8, the pressure coefficient is very slightly influenced by the choice of the equation of state of the fluid around the airfoil, indicating a low influence of the equation of state on aerodynamical properties of the considered flow. The temperature of the airfoil (different for each configuration a: 1500K, b: 1000K, c: 300K) does not influence the results of the pressure coefficient, which is the same for each configurations. A few changes are visible on the trailing edge,

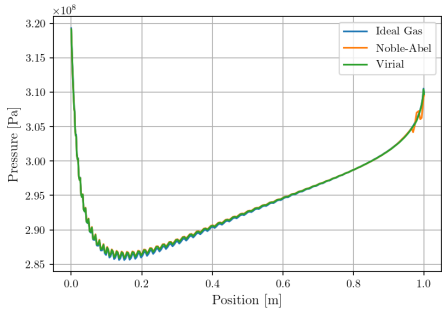

FIG. 6. Pressure as a function of position along the wing profile for the ideal gas equation, comparison with data from the literature[27,28] (similar magnitude of Reynolds number 10^6). Mach number: 0.3, temperature of the airfoil: 300K.

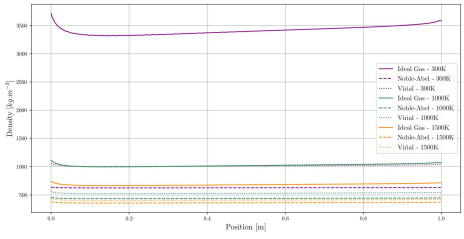

FIG. 7. Density as a function of position along the wing profile for the ideal gas equation, comparison with data from the literature[27,28] (similar magnitude of Reynolds number 10^6). Mach number: 0.3, temperature of the airfoil: 300K.

but they are purely numerical.

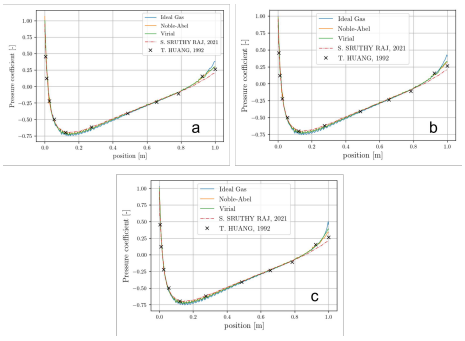

FIG. 8. Pressure coefficient(31) around the airfoil (NACA 0020) for Ideal gas, Noble-Abel and virial equations, depending on the configurations (a: 1500K, b: 1000K, c: 300K)/ Re $= 5 \cdot 10^6$, Mach number 0.3.

The drag effects have also been studied for each equation of state and each configuration. The forces of friction along the x-axis integrated on the surface of the foil are presented for the pressure contribution and for the shear contribution in table VI, depending on the equation of state and the configuration. The pressure contribution is predominant, one order of magnitude higher in comparison with shear friction force. The total values of friction, sum of the pressure and shear contribution, are quite different depending on the equation of state : around 40% between ideal gas and the others for configuration all configurations (ideal gas being the reference). The final values also fluctuates a lot due to numerical oscillations as explained before, giving a high values of uncertainties. Figure 9 illustrates the resulting force for each configuration and equation of state, along with the associated uncertainties (one standard deviation).

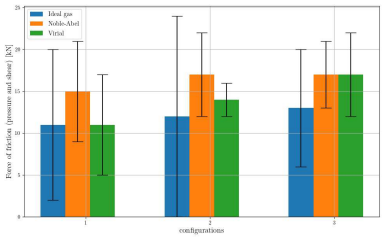

FIG. 9. Forces of friction projeted along the x-axis (pressure and shear contributions) around the airfoil (NACA 0020) for Ideal gas, Noble-Abel and virial equations, depending on the configurations (1: 300K, 2: 1000K, 3: 1500K)/ Re $= 5 \cdot 10^6$, Mach number 0.3.

3. Heat flux

Table VII presents the mean heat flux (on the last 1000 iterations) for each configuration and each equation of state, with associated numerical uncertainties (one standard deviation).

The heat flux (32) is a function of the density, which is strongly influenced by the choice of the equation of state, as seen section III 2. Indeed, the density predicted by the ideal gas equation is up to three times larger than the density predicted by other equations of state (configuration 1). This explains the major difference between the predictions of heat flux as a function of the equation of state. This difference is particularly pronounced for configuration 1, where the density varies widely depending on the choice of the EOS.

Figure 10 presents the values of the heat flux coefficient, depending on the equation of state and the configuration of the simulation. The standard deviation is also plotted (statistical value on the last 1000 iterations). The

TABLE VI. Force along x-axis integrated around the airfoil, mean values on the last 1000 iterations for each configuration (temperature of the foil: 300K, 1000K and 1500K) and equation of state (Ideal gas, Noble-Abel and virial), contribution of the pressure and the shear (viscosity effects).

Equation of state	Force (x-axis) configuration 1 Pressure / Shear (kN)	Force (x-axis) configuration 2 Pressure / Shear (kN)	Force (x-axis) configuration 3 Pressure / Shear (kN)
Ideal Gas	8.7 / 2.3	10 / 1.1	12 / 0.6
Noble-Abel	14 / 0.7	14 / 0.5	17 / 0.4
Virial	9.7 / 0.9	14 / 0.6	17 / 0.5

TABLE VII. Heat flux integrated around the airfoil, mean values on the last 1000 iterations for each configuration (temperature of the foil: 300K, 1000K and 1500K) and equation of state (Ideal gas, Noble-Abel and virial), with numerical uncertainties (one standard deviation).

Equation of state	Heat flux configuration 1 (MW)	Heat flux configuration 2 (MW)	Heat flux configuration 3 (MW)
Ideal Gas	32 ± 1.4	11 ± 0.7	4.6 ± 0.7
Noble-Abel	11 ± 0.7	6.0 ± 0.6	3.1 ± 0.5
Virial	13 ± 1.0	6.3 ± 0.6	3.3 ± 0.6

results clearly highlight a variation of the heat transfer coefficient with the equation of state for each configuration. The ideal gas predictions are highly above the predictions of Noble-Abel and virial, whereas virial and Noble-Abel are relatively close. For the first configuration (airfoil's temperature: 300K) the difference between ideal gas is up to three times higher than Noble-Abel and virial. This result decreases with configuration 2 and 3 (respectively airfoil at 1000K and 1500K) with ideal prediction twice higher than virial and Noble-Abel for configuration 2 and 50% difference for configuration 3. The difference between Noble-Abel and the virial is moderated, around a few percent. These variations are explained by the difference observed on the predicted density depending on the equations of state simulated. Indeed, the heat flux (32) is a linear function of the density in the configurations simulated, and the differences observed on the heat flux are the same observed for the density around the airfoil. As the choice of the equation of state impacts the numerical prediction of the density, is has also repercussion on the numercial heat flux integrated around the airfoil.

As seen in this section, the aerodynamical properties of a NACA 0020 profile in a flow at interior ballistics conditions is unchanged by the choice of the equation of state. However, the choice of the equation of state has a strong influence on the numerical prediction of the heat transfer for the considered case, in particular when the fluid is in a state where the ideal gas assumptions are not valid anymore. The variations of the density depending on the equation of state are responsible for the variations observed numerically, as the heat flux is function of the density and it is the only variable changing with the equation of state. Therefore, the prediction of heat flux is impacted by the choice of the equation of state, as the density depends strongly on it.

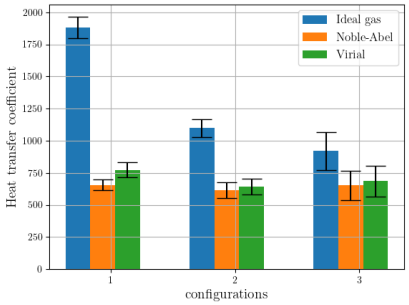

FIG. 10. Heat flux coefficient (33) around the airfoil (NACA 0020) for Ideal gas, Noble-Abel and virial equations, depending on the configurations (1: 300K, 2: 1000K, 3: 1500K)/ Re $= 5 \cdot 10^6$, Mach number 0.3.

IV. INTERIOR BALLISTICS APPLICATION

The gaseous mixture considered in interior ballistics is produced by the combustion of a propellant (energetic material), such as nitrocellulose, double base propellant... Its composition is therefore complex, both because there are more than two components and because of the nature of the components involved.

1. From air to combustion products

The exact composition depends on the burnt energetic material. Generally, combustion products are composed

of dozens of components. However, it is possible to consider only the main components (in mass or molar fraction), with reasonable accuracy. The difficulty remains in knowing the exact composition of the mixture for a given propellant (molecules and mass fraction). Indeed, the composition depends on the propellant studied. Generally, a thermochemical software is needed to obtain this information. Most software relies on the principle of minimization of free energy (Gibbs' Energy)[15]. The main components of combustion products are: NO_2, NO, CO, CO_2 and H_2O. The confidentiality of the mixtures studied is also an issue, as few information are available in the literature on the exact components and quantities of the molecules composing the gas. The results presented in this paper are considered for a propellant taken from the literature[33]. A similar method can be applied for a given propellant, provided that all the information needed are known. Another difficulty, in comparison with air, is the different nature of the components. Indeed, some are polar molecules (such as water, which is a major component of combustion products), so in that case the intermolecular potential used for the virial calculation is the Stockmayer potential (instead of the Lennard-Jones potential used for non-polar molecules). The Stockmayer potential implies the knowledge of one more parameter (dipolar moment μ), which is known with an uncertainty of 10%. The calculations are detailed in[1,15,16] and are not reproduced in this paper, but it should be noted that the calculations for polar molecules are more tedious than for non-polar molecules, with more uncertainties. The method also adds uncertainties of the values of the virial coefficients (B and C) with the introduction of the dipolar moment, which widen the range of uncertainties of the virial equation in comparison with air. The covolume of combustion gases can be determined experimentally, with closed vessel tests, so called Amagat's method. This method is not as precise as the calculation with critical pressure and critical temperature, but the uncertainties remain around a few percent (uncertainties of sensors). Thermochemical software is also an option to calculate the covolume (calculations with critical pressure and temperature), however the uncertainties on the covolume given by software are not well known. The uncertainties around the Noble-Abel equation are then slightly wider than for air, but they remain slimmer than the uncertainties of the virial equation.

2. Application to a propellant from the literature

The propellant studied is extracted from the literature[33] and is composed of nitrocellulose. The main components are given table VIII from[33], along with their molar fraction (HCN and CH_2O have been neglected regarded their low molar fraction). Polar molecules are precised (use of the Stockmayer potential instead of the Lennard-Jones potential). The temperature of the calculation is the flame temperature (3000 K). The covolume is estimated[34] at $1.11 \cdot 10^{-3} m^3 \cdot kg^{-1}$.

TABLE VIII. Molecules composing the combustion products of the considered propellant[33], along with their molar fraction and parameters σ and ε needed for the virial coefficients calculations.

Components	Molar fraction (%)	σ (nm)	$\frac{\varepsilon}{k}$(K)
N_2	4	0.358	118
CO	42	0.376	100
CO_2	10	0.407	205
NO	14	0.317	131
H_2	4	0.293	37
H_2O[a]	24	0.256	380

[a] polar molecule

It is then possible to calculate the virial coefficients for each component of the gas, using equations (10) and (12). Table IX summarizes the values of B and C for each component and the resulting mixture (simple mixture law, equations (13) and (14)). Figure 11 is a plot of both Noble-Abel and virial equations for the combustion gases produced by nitrocellulose.

TABLE IX. Molecules commposing the combustion products of the considered propellant[33], along with their virial coefficients and the resulting virial coefficients for combustion products.

Components	B $(m^3 \cdot kg^{-1})$	C $(m^6 \cdot kg^{-2})$
N_2	$1.20 \cdot 10^{-3}$	$1.12 \cdot 10^{-6}$
CO	$1.26 \cdot 10^{-3}$	$1.26 \cdot 10^{-6}$
CO_2	$0.98 \cdot 10^{-3}$	$0.99 \cdot 10^{-6}$
NO	$0.71 \cdot 10^{-3}$	$0.43 \cdot 10^{-6}$
H_2	$7.59 \cdot 10^{-3}$	$3.89 \cdot 10^{-5}$
H_2O[a]	$0.42 \cdot 10^{-3}$	$0.65 \cdot 10^{-6}$
Combustion products	$\mathbf{0.90 \cdot 10^{-3}}$	$\mathbf{1.12 \cdot 10^{-6}}$

[a] polar molecule

Regarding uncertainties, interval analysis has once again been used to compute the uncertainties on the coefficients of Noble-Abel and the virial. The method used is the same as described in section II 3 for air. The uncertainties on the virial coefficient are on σ and epε, parameters of the intermolecular potential. For polar molecules, water vapor in the presented case, an extra 5% is added on the polar molecule (so 15% of uncertainties on B and C for water), to account for the tabulation and interpolation used for the calculations. The uncertainty of the covolume is estimated to be 1%, as the value has been chosen in the literature and is probably determined experimentally with closed vessel test. Table X presents the uncertainties of Noble-Abel and virial coefficients for combustion products (composition given table VIII) at 3000K.

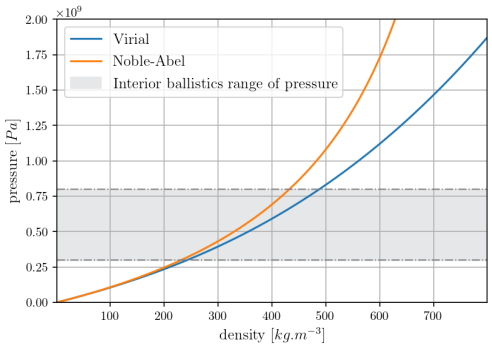

FIG. 11. Pressure as a function of density for combustion products at 3000K predicted by different equations of state (Noble-Abel and virial). Coefficients for the EOS are given in table IX for virial. The grey area highlights the pressure range commonly considered in interior ballistics applications

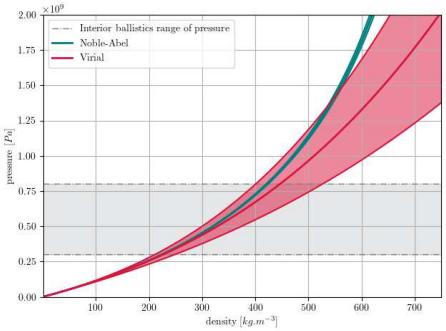

FIG. 12. Pressure as a function of density for combustion products at 3000K predicted by different equations of state (Noble-Abel and virial), along with their respective intervals of uncertainties, as given in table X. The grey area highlights the pressure range commonly considered in interior ballistics applications.

TABLE X. Interval of uncertainties of the coefficients of the EOS (covolume for Noble-Abel, B and C for the virial), calculated with interval arithmetic for combustion products of literature propellant[33] at 3000K.

Coefficients of EoS	Interval of uncertainties
Covolume $(m^3 \cdot kg^{-1})$	$[1.09; 1.12] \cdot 10^{-3}$
B $(m^3 \cdot kg^{-1})$	$[0.66; 1.41] \cdot 10^{-3}$
C $(m^6 \cdot kg^{-2})$	$[0.58; 2.61] \cdot 10^{-6}$

Figure 12 presents the results obtained with the virial and Noble-Abel equations, with their intervals of uncertainties, given in table X, for the mixture studied (representative of combustion products, in table VIII). For combustion products, the results derived with the Noble-Abel equation of state and their range of uncertainties are included in the range of uncertainties of the results obtained with the virial equation over the whole range of pressure encountered in interior ballistics. The conclusions are then slightly different than for air, as long as the pressure is in the actual range of pressure of interior ballistics. The Noble-Abel equation seems to be a good option, as the uncertainties on the virial equation are too large for an interior ballistics application. However, no experimental points are available for combustion products. This lack of validation affects the conclusions, as the exact behavior of the gases is unknown, precluding the choice of the most appropriate equation of state. Considering the extreme conditions encountered in interior ballistics, an experimental validation is difficult to set up and considering the defense application, the literature is not extensive on the subject.

V. CONCLUSION

In definitive, the choice of an equation of state adequate for intermediate level of pressure encountered in interior ballistics is not obvious. There are two potential candidates: Noble-Abel, which remains simple (only one coefficient, easily accessible and with low uncertainties) but exhibits a non physical behavior when the pressure rises. The virial equation has a more physical description and is the closest to the few experimental data in the literature for air (SESAME database[18]), but its coefficients are difficult to calculate and have high uncertainties. Furthermore, the numerical study highlighted that the equation of state is not only responsible for the predictions of thermodynamical properties, but also thermical properties. Indeed, for instance the prediction of the numerical heat flux depends on the choice of the equation of state. It is therefore crucial to choose the accurate equation of state. The conclusion drawn for air applied also for combustion products, namely that the Noble-Abel equation seems to be the best compromise for an interior ballistics application, with pressure under 700 MPa. However, this conclusion could be reviewed with the development of new high-pressure weapon. In that case, the virial equation might become a better choice and the method for determining its coefficients should be revised to decrease their uncertainties.

ACKNOWLEDGMENTS

The authors thank CTA International and the French Ministry of Defense (Agence de l'Innovation de Défense) for the financial support of this work (PhD Thesis –

AID/ANRT 2020862). The authors thank also Scott CROCKETT from LANL (Los Alamos National Laboratory) for the delivery of the SESAME database.

DATA AVAILABILITY STATEMENT

The data that support the findings of this study are available from the corresponding author upon reasonable request.

VI. APPENDICES

This part detailed the expression needed to manually implemented equations of state in CFD softawre, such as STARCCM+©. The code needs the density and both derivatives of the density relatively to the pressure and the temperature.

Thus, for Noble-Abel (36, 37 and 38):

$$\rho = \frac{P}{rT + \eta P} \tag{36}$$

$$\frac{d\rho}{dP} = \frac{rT}{(rT + \eta P)^2} \tag{37}$$

$$\frac{d\rho}{dT} = \frac{-rP}{(rT + \eta P)^2} \tag{38}$$

For the virial equation, the calculations are far more arduous. Indeed, the density is the only real and positive solution of a third order equation (7). The Cardan's formulas have then been used to find the expression of the density (39) from the virial equation.

$$\begin{aligned}\rho = &-\frac{B}{3C} \\ &-\frac{(3C - B^2)\cdot 2^{1/3}}{3C(-2B^3 + 9BC + \frac{27C^2P}{rT} + (4(3C - B^2)^3 + (-2B^3 + 9BC + \frac{27C^2P}{rT})^2)^{1/2})^{1/3}} \\ &+\frac{(-2B^3 + 9BC + \frac{27C^2P}{rT} + (4(3C - B^2)^3 + (-2B^3 + 9BC + \frac{27C^2P}{rT})^2)^{1/2})^{1/3}}{3C\cdot 2^{1/3}}\end{aligned} \tag{39}$$

$$\frac{d\rho}{dP} = \frac{1}{rT(1 + 2\cdot B\rho + 3\cdot C\rho^2)} \tag{40}$$

$$\frac{d\rho}{dT} = \frac{-r\cdot(\rho + B\rho^2 + C\rho^3)^2}{P(1 + 2\cdot B\rho + 3\cdot C\rho^2)} \tag{41}$$

REFERENCES

[1] J. Hirschfelder, C. Curtiss, and R. Bird, *Molecular theory of gases and liquids* (John Wiley and Sons, 1964).
[2] R. Menikoff, "Jwl equation of state," Tech. Rep.
[3] S. Wang, P. Butler, and H. Krier, "Non-ideal equations of state for combusting and and detonating explosives," Progress in energy and combustion science **11**, 311–331 (1985).
[4] C. Tarver and E. McGuire, "Reactive flow modeling of the interaction of tatb detonation waves with inert materials," Tech. Rep. (Lawrence Livermore National Lab.(LLNL), Livermore, CA (United States), 2002).
[5] S. Amar, E. Kochavi, Y. Lefler, S. Vaintraub, and D. Sidilkover, "Comparison of bkw and jwl equations of state for explosion simulations," in *30th International Symposium on Shock Waves 2: ISSW30-Volume 2* (Springer, 2017) pp. 1003–1008.
[6] D. Carlucci and S. Jacobson, *Ballistics: theory and design of guns and ammunition* (CRC Press, 2018).
[7] J. Corner, *Theory of the internal ballistics of gun* (John Wiley and Sons, 1950).
[8] R. Gemerschausen, *Handbook on Weaponry*, rheinmetall ed. (1982).
[9] NATO-Organisation, "Stanag 4367: Thermodynamic interior ballistics model with global parameters," (1997).
[10] L. Neron and R. Saurel, "Noble-abel/first-order virial equations of state for gas mixtures resulting from multiple condensed reactive materials combustion," Physics of Fluids **34**, 016107 (2022).
[11] Y. Ma, F. Nan, and W. He, "Corrected internal ballistic simulation of high chamber pressure gun," IOP Conference Series: Materials Science and Engineering **439** (2018).
[12] F. Volk and H. Bathelt, "Application of the virial equation of state in calculating interior ballistics quantities," Propellants, Explosives, Pyrotechnics **1**, 7–14 (1976).
[13] M. Munoz, "Norme nf t70-714 tirs enceinte manométrique," Norme (2004).
[14] G. Soave, "Improvement of the van der waals equation of state," Chemical engineering science **39**, 357–369 (1984).
[15] NATO-Organisation, "Stanag 4400: Derivation of thermochemical values for interior ballistic calculations," (1993).
[16] M. Brateau, A. Bouchama, A. Clough, I. Delagrange, S. Kerampran, and M. Arrigoni, "Evaluation of existing equations of state for the modelling of propellant combustion in interior ballistics," in *32nd International Symposium on Ballistics* (2022).
[17] R. Sevast'yanov and R. Chernyavskaya, "Virial coefficients of nitrogen, oxygen, and air at temperatures from 75 to 2500 k," Journal of engineering physics **51**, 851–854 (1986).
[18] S. Lyon and J. Johnson, "T-1 handbook: The sesame equation of state library - vol. 1&2," Tech. Rep. LA-CP-98-0100. (Los Alamos National Laboratory, 1998).
[19] E. W. Lemmon, R. Jacobsen, S. Penoncello, and D. Friend, "Thermodynamic properties of air and mixtures of nitrogen, argon, and oxygen from 60 to 2000 k at pressures to 2000 mpa,"

Journal of physical and chemical reference data **29**, 331–385 (2000).
[20]R. Jacobsen, R. Stewart, and M. Jahangiri, "Thermodynamic properties of nitrogen from the freezing line to 2000 k at pressures to 1000 mpa," Journal of Physical and Chemical Reference Data **15**, 735–909 (1986).
[21]W. Wagner, J. Ewers, and W. Pentermann, "New vapour-pressure measurements and a new rational vapour-pressure equation for oxygen," The Journal of Chemical Thermodynamics **8**, 1049–1060 (1976).
[22]C. M. d. Thermodynamics Research Center, NIST Boulder Laboratories, "Thermodynamics source database," Tech. Rep. (2022).
[23]R. Moore, R. Kearfott, and M. Cloud, *Introduction to interval analysis* (SIAM, 2009).
[24]R. Moore, *Methods and applications of interval analysis* (SIAM, 1979).
[25]H. Graboske, "New eos for air," Tech. Rep. (California Univ., Livermore (USA). Lawrence Livermore Lab., 1975).
[26]J. McDevitt and A. Okuno, "Static and dynamic pressure measurements on a naca 0012 airfoil in the ames high reynolds number facility," (1985).
[27]S. Raj, H. Krishna, M. Issac, and D. Ebenezer, "Numerical analysis of wall shear stress, pressure, drag and lift of the naca 0020 airfoil used in darpa suboff," (2021).
[28]T. Huang and H. Liu, "Measurements of flows over an axisymmetric body with various appendages in a wind tunnel: the darpa suboff experimental program," (1994).
[29]S. Sadaq, S. Mehdi, S. Mehdi, and S. Yasear, "Analysis of naca 0020 aerofoil profile rotor blade using cfd approach," Materials Today: Proceedings **64**, 147–160 (2022).
[30]C. Jayatilleke, "The influence of prandtl number and surface roughness on the resistance of the laminar sub-layer to momentum and heat transfer," (1966).
[31]P. Kosky, R. Balmer, R. Balmer, W. Keat, and G. Wise, *Exploring engineering: an introduction to engineering and design* (Academic Press, 2012).
[32]N. Azzedine and B. Lakhdar, "Compressibility effects on distributions of pressure and lift coefficients," Sciences& Technology Vol 2 – N°1 , pp19–23 (2017).
[33]T. Jensen, J. Moxnes, E. Unneberg, and O. Dullum, "Calculation of decomposition products from components of gunpowder by using reaxff reactive force field molecular dynamics and thermodynamic calculations of equilibrium composition," Propellants, Explosives, Pyrotechnics **39**, 830–837 (2014).
[34]Y. Chen, M. Chen, L. Zhang, R. Zhao, and J. Wen, "Combustion characteristic parameter testing and caculating of single-base propellant," in *Advanced Materials Research*, Vol. 1006 (Trans Tech Publ, 2014) pp. 185–187.